Environmental Fluid Mechanics
https://doi.org/10.1007/s10652-019-09707-8

ORIGINAL ARTICLE

Numerical modelling of uncongested wood transport in the Rienz river

Elisabetta Persi[1,2] · Gabriella Petaccia[1] · Stefano Sibilla[1] · Ana Lucía[3] · Andrea Andreoli[4] · Francesco Comiti[4]

Received: 4 December 2018 / Accepted: 26 June 2019

Abstract
The Eulerian–Lagrangian model ORSA2D_WT is employed for the simulation of uncongested wood transport, with reference to a field experiment that studied the motion of regular and unbranched cylindrical wooden samples. The model calculates the entrainment, transport and deposition of large wood elements by computing the hydrodynamic forces exerted by the flow. The experimental log positions and displacements are taken as a reference for the first application of the numerical model to a real-scale test case. Special attention is paid to the presence of large boulders, which interact with floating wood and are represented as nearly 3D elements in the numerical domain, to take into account their effect both on the flow and on the logs. The comparison between the field data and the numerical simulation shows that the model fails to replicate exactly each log trajectory. However, when the focus moves to the behaviour of the entire group of logs, the model appears to simulate quite well the areas where logs are more prone to stop. The wood density implemented in the model strongly affect the results in terms of single log displacement, emphasizing the importance of the correct estimation of this parameter for large wood simulation.

Keywords Large wood transport · Discrete element model · Wooden log arrest · Uncongested transport

1 Introduction

In stream wood pieces have a positive impact on the aquatic ecosystem, since they can contribute to the formation of a variate geomorphology [3, 34] providing nutrient and suitable habitat for fish and other aquatic fauna [11]. However, several hydraulic issues are related to the presence of wood and to its accumulation upstream of bridge piers [14, 42]

✉ Elisabetta Persi
elisabetta.persi@unipv.it

1 DICAR, University of Pavia, Pavia, Italy

2 Present Address: DICAM, University of Trento, Trento, Italy

3 Department of Geosciences, University of Tübingen, Tübingen, Germany

4 Faculty of Science and Technology, Free University of Bolzano, Bolzano, Italy

especially under high flow conditions. Span clogging and resulting backwater effect or bridge overflow may endanger urban areas [37] and local bed erosion induced by altered flow field at bridge piers may be critical for structures stability [20].

Due to the above mentioned risk, a comprehensive approach for flood risk mitigation should be adopted with appropriate integrated management strategies [21, 25, 26] that take into account the effect of woody material on hydraulic risk. All the processes that contribute to wood transport, like the estimation of the available wood volumes [15, 38] or the description of wood dynamics, should be carefully analysed to become part of an integrated approach. In this framework, experimental [4, 6, 12, 35] and theoretical [5] insights for the assessment of large wood entrainment and transport are analysed in the literature, pointing out the connections between wood motion and the geometrical characteristics of logs, of channel hydraulics and of the river morphology. The interaction with in-stream structures, such as bridge piers, decks or retention structures, needs also to be considered for the evaluation of flood risk [13].

The advancement of knowledge in wood-related issues is the starting point for the development of numerical models that can help in limiting the hazard associated to large wood. Existing models couple the solution of the flow field with the computation of logs motion, which might be modelled considering the transport of an established volume of wood based on the 2D flow field [25], or calculating the displacement of single logs, either with a kinematic [36] or a dynamic approach [1, 28, 44]. Bridge or check dams clogging is one of the most critical aspects for modelling, since it presents random features which need to be combined to the deterministic aspects of wood transport. Current attempts of simulating wood and structure interaction include the combination of physically-based models with stochastic approach [24], 2D strategies that put together flume experiments and the estimation of blocking probability [36, 43] and even 3D modelling strategies [19].

The application of these models to real-scale events [40] requires not only reliable numerical strategies, but also several information about the logs and basin characteristics. Up to now, cylindrical logs are considered, although some attempts of including the effects of rootwads and branches are found both in experimental and numerical studies [7, 9]. Log length, diameter and density are often related to the dimensions of wood in the surrounding area [40]. The knowledge of the flow hydrograph, together with the number of involved wood pieces and their length, are essential for the estimation of the blockage probability [41]. Adequate domain discretization and surface roughness are also needed, which may require specific field survey to integrate available elevation models or aerial images.

An attempt to provide a nearly complete set of information is found in [2, 23], where a field experiment carried out in a sub-reach of the Rienz river is analysed. The Rienz/Rienza River is a tributary of Eisack/Isarco river in South Tyrol (Northern Italy), and was already involved in an attempt of integrated hazard mapping procedure [24] that included the effect of bridge clogging due to the interaction of wood and sediments. In addition, upstream the city of Bruneck/Brunico two trapping structure, a check dam and a rope net, were installed [22] to avoid bridge clogging within the city. In this context, the field experiment was performed to evaluate the mobility of unbranched logs in a reach upstream of the city of Bruneck, providing information about logs motion in relation with the local flow conditions.

This experiment is here employed to assess the capabilities of the Eulerian–Lagrangian model ORSA2D_WT for the simulation of large wood transport under real-scale conditions. The model adopts a dynamic strategy for the simulation of wood transport, i.e. log motion is computed from the hydrodynamic forces exerted by the flow. It includes the drag and side forces, with proper hydrodynamic coefficients [30], and the added mass and

pressure gradient components. The Lagrangian part is one-way coupled with an Eulerian finite volume first order accurate Shallow Water Equation (SWE) solver. The final code was calibrated on laboratory flume experiments for floating dowels transport [29] while this first application to a real-scale case study is the opportunity to assess the model performances verifying (i) the influence of the logs characteristics (i.e. density and dimension) on the simulation of wood transport and (ii) the accuracy of the model in replicating large wood displacement in a real environment, where the interaction with the domain may play a significant role.

2 Methodology

2.1 Test description

The field experiment described in [2, 23] covered the period May 2011–November 2014, with periodical measurement of the log displacement and continuous monitoring of flow discharge.

For the simulation, a sub-reach of the originally surveyed part was selected (Fig. 1a). The reach is 1.8 km long, has an average slope of 0.9%, a width in the range 7–12 m and is located downstream of the Monguelfo dam, about 6 km upstream of the city of Bruneck. In total, 133 tagged cylinders were placed either aligned, perpendicular or at 45° with respect to the local cross section. Among them, 83 were introduced on purpose thanks to the collaboration of the Department of Hydraulic Engineering of the Autonomous Province of

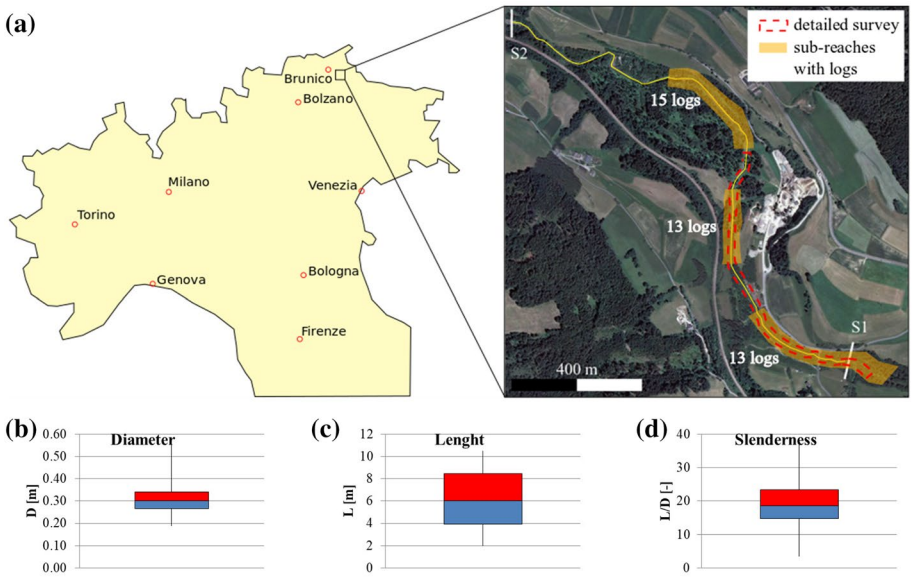

Fig. 1 **a** Location of the Rienz river and enlarged panel with the extension of the reach used for the numerical simulation; pressure transducer in section S1; final section S2; coloured areas show where logs are located, with corresponding number of logs; **b** distribution of log diameter; **c** distribution of log length; **d** distribution of log slenderness

Bozen/Bolzano while the remaining 50 were natural logs found in the river. A pressure transducer was installed in the upstream section (S1 in Fig. 1) to monitor continuously the water level and obtain a relation among wood mobility and hydraulic variables.

The most important displacements of the tagged logs in this sub-reach occurred in the period from June 26th to July 5th, 2012, which was selected for the simulation with ORSA2D_WT. On June 26th, 35 logs were located in the reach, distributed in three sub-reaches as shown in Fig. 1a, with lengths ranging from 2 to 10.5 m and diameter from 0.20 to 0.55 m. The distribution of logs characteristics is shown in Fig. 1b–d for diameter, length and slenderness respectively. Most of the diameters are in the range 0.28–0.34 m, with few elements out of the 2nd and 3rd quartiles, while an evenly distributed variation of the cylinders length is observed around the average value of 6 m. Minimum dimensions are larger than the minimum conventional sizes characterising large wood (1 m length and 0.1 m diameter, [18]). The range of diameters was representative of the characteristics of the vegetation found in the floodplain, while the logs length was adjusted to have uniform classes of length ranging from the average channel width to $1/4-1/5$ of this value.

The water depth hydrograph (Fig. 2a), measured at the gauged section S1 in the period between June 26th and July 5th 2012 shows two peaks, which are related to management operations at the Monguelfo dam located just upstream.

The rating curve of the Rienz river was estimated combining the water depth and discharge measurements obtained during the experimental campaign (for low discharge event, around 3.2 $m^3\ s^{-1}$) including the data of two heavy rain events, which occurred on November 5th and 11th 2012. In that period, a malfunction of the pressure transducer prevent the measurement of the water level in section S1, hence the measurements performed during the field surveys in other sections are employed as a reference. Discharge values of the tributaries and of the environmental flow released by the dams were provided by the Province of Bolzano and used to estimate the discharge of the Rienz river.

Figure 2b shows the logarithmic interpolation of the available data superimposed to the discharges calculated for the peak events observed in the period considered for the simulation: $h = 0.50$ m and $Q = 5.53\ m^3\ s^{-1}$ on June 27th and $h = 0.62$ m and $Q = 6.44\ m^3\ s^{-1}$ on July, 4th. These two events are implemented in ORSA2D_WT to simulate the flow condition for large wood transport.

The initial and final log positions were taken by the survey data-sheet form the experimental campaign described in [2, 23]. Log orientation was recorded as parallel,

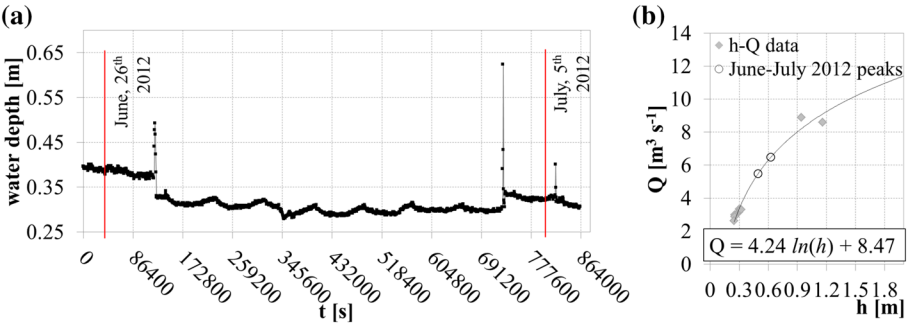

Fig. 2 **a** Water level hydrograph covering the period between the field surveys, on June 26th and on July 5th, 2012; **b** rating curve for the Rienz river and peak discharges for the two peak events implemented in the simulation

perpendicular or oblique, but no additional details were provided about the exact log-section angle for the latter case. The logs were found in the river or laying on the banks, and in some cases were partially submerged or stuck against other obstacles (rootwads, other logs, riverine vegetation or boulders).

The experimental data shows that logs tend to stop at large boulders and that the local singularities of the cross section, as riffles or fallen trees, affect the log motion. For this reason, an additional detailed survey was carried out with the aim of getting an accurate description of the channel and of locating large obstacles and recording their extension and height, integrating the survey already performed [2, 23]. A river reach of 800 m was surveyed with a total station and GPS, focusing on the middle part of the reach (red dashed line in Fig. 1a) where log movement was the most evident. Over 60 large boulders were found, with an average planar dimension varying from 0.5 to 1.3 m and an average height above the river bed of 0.35 m. Boulders were nearly equally grouped in 2 reaches, located from 450 to 650 m and from 840 to 910 m from the initial section, respectively; the respective boulder density in the two reaches was 0.15 and 0.43 boulders per meter along the channel axis.

2.2 Numerical simulation

ORSA2D_WT can simulate large wood entrainment, transport, rotation and deposition, as well as the interactions that may occur between wooden elements and with in-stream obstacles. The hydrodynamic module solves the SWE with a first order, upwind finite volume scheme; it was applied to simulate natural flood waves, as well as dam break waves [31, 32]. The Discrete Element dynamic subroutine of ORSA2D_WT computes log motion only if the logs are able to float. This condition is verified with a formulation derived from the analysis proposed in [5], which balances the effect of gravity and the drag force (favourable to wood motion) with the friction force. The friction coefficient implemented in the code varies from static to dynamic for incipient motion or arrest conditions, respectively. If the logs float, they move on the water surface and rotate on the horizontal plane based on the forces computed at four points around the centre of mass. The forces included in the model are the drag and side force, with appropriate hydrodynamic coefficients that vary according to log orientation [30], the added mass force and the pressure gradient. Basically, the effects of flow hydrodynamics and differential acceleration are included and used to compute log motion. Interactions among logs and with other obstacles are calculated with a kinematic condition [17], with an elastic coefficient calibrated for the collision of bodies surrounded by water.

A schematic explanation of the model equation is shown in Fig. 3. More details about the numerical model can be found in [27–29, 33].

Data needed by ORSA2D_WT are the domain topography and roughness, the initial and boundary conditions for both the hydraulic and the large wood transport simulations (inlet discharge, outflow condition, log number, positioning, dimension and wood density).

The physical domain is obtained by a DTM provided by the Autonomous Province of Bozen/Bolzano, which has a resolution of 2.5 m. For the riverbed, the DTM was integrated with the cross sections surveyed during the periodical monitoring in [2, 23] and with the results of the detailed survey carried out on April 2015 which provided the location and sizing of in-channel boulders. Thanks to the detailed survey, the implemented geometry presents a level of accuracy which is higher than the standard domain normally employed for numerical simulations. In particular, the presence of boulders in the stream

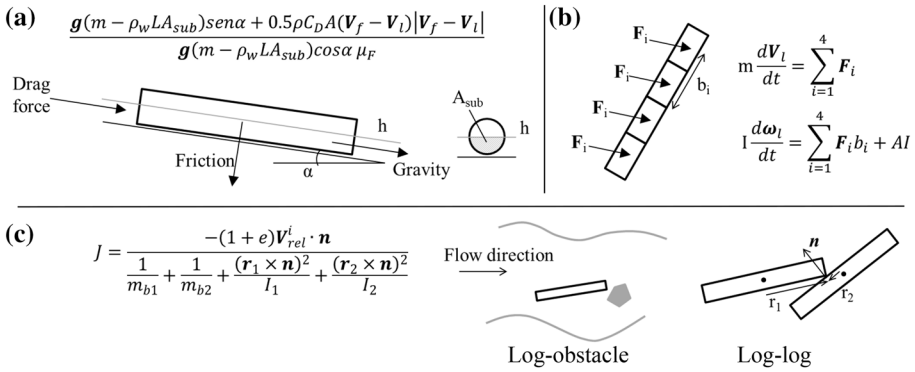

Fig. 3 **a** Entrainment model: $\boldsymbol{g}$ gravitational acceleration, m log mass, ρ_w water density, C_D drag coefficient, A log longitudinal area, $\boldsymbol{V}_f$ flow velocity, $\boldsymbol{V}_l$ log velocity, L log length, μ_F friction coefficient; **b** planar translation and rotation model: $\boldsymbol{F}_i$ local forces in x and y direction, including drag force, side force, added mass and pressure gradient, I log moment of inertia, ω_l log angular velocity, AI added inertia term [29]; **c** collision model: J impulse momentum, which represents the loss/gain of energy due to the collision, e restitution coefficient, $\boldsymbol{V}^i_{rel}$ relative velocity at the contact point, $\boldsymbol{n}$ normal unit vector at the contact point

was carefully detected, since many logs in the experimental campaign were found anchored at boulders (29% of logs, while the 14% were anchored at trees). An unstructured triangular grid was adopted, made of over 51800 elements having different areas according to their proximity to the riverbed, with cell edge lengths ranging from 5 m in the outer part to 2.5 m in the main channel. Local refinement was also introduced to include boulders, which are represented as nearly 3D obstacles. To represent boulders, cells with an average size ranging from 0.4 to 1.5 m were employed for the reach where the boulders were found, and one common vertex was lifted in order to represent the real height of the stone. Boulders result hence as solid pyramids, with at least three edges, as shown in Fig. 4b.

The Manning coefficient n is used to represent bed roughness. For the river bed, in order to quantify the bed roughness relevant for large wood transport, the spatial density of boulders (diameter > 25 cm) and their dimensions were measured for each homogeneous reach during the previous field experiments [23]. The mean axis of the boulders was measured with a tree caliper in a squared area around the cross sections covering the entire width

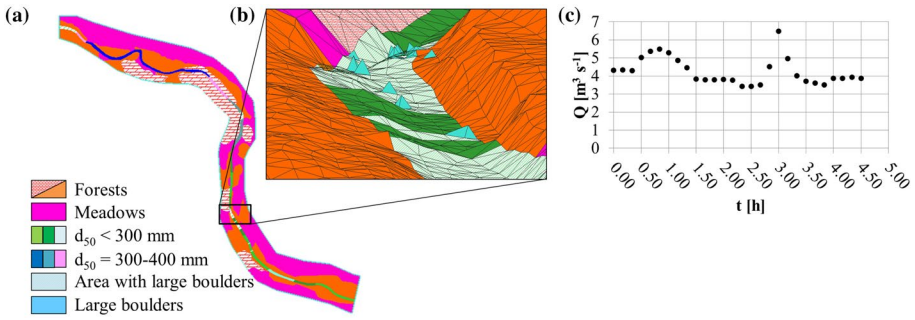

Fig. 4 **a** Top view of the mesh. Different colours refer to different Manning coefficients, resumed in Table 1; **b** magnified view of the boulders as pyramidal solids; **c** discharge hydrograph used as upstream boundary condition in the simulation

and an equivalent length parallel to the flow. In case the number of measured boulders was smaller than 30, the length of the measured area was increased in order to have at least 30 boulders inside. The dimensions of this area was measured with a rangefinder. The boulder size is used to estimate the riverbed roughness with Cowan method [10], selecting a base value based on $d50$ which is then modified according to the characteristics of the sub-reach (slope, curves, vegetation). Employing the boulder size instead of the surface grain size may lead to some inaccuracies in the estimation of the roughness coefficient, but the values obtained are in agreement with the overall situation of the riverbed. Note that for areas with large boulders ($d50 > 60$ cm) a higher value is assigned, to take into account the effect of macro-roughness elements. For the flood plain and the forested areas, values suggested in [8] are used, based on visual identification of geo-referenced aerial image of the domain and the performed survey. The chosen values are shown in Table 1, and the subdivision of areas with different roughness is displayed in Fig. 4a.

As the water stage hydrograph (Fig. 2b) shows that the peaks follow a relatively long period when the water depth in the initial section is constant, the initial condition is preliminarily obtained running a steady-state simulation with $Q = 4\,\mathrm{m^3\,s^{-1}}$ and, then, the transient flow with log displacement is simulated with the upstream discharge hydrograph shown in Fig. 4c, starting from stationary conditions. The two peaks occurring in the considered period are simulated as subsequent flood-waves, in order to reduce the computational time. This assumption is possible since, between the two peaks, the logs do not move due to the reduced water level, so no underestimation of log displacement derives from the shortening of the hydrograph. The downstream boundary condition is set as the critical depth, since the final section is located just upstream of a step.

To simulate wood transport, the model requires the number of logs, their dimension, initial position (mass centre) and orientation. Another important variable is the wood density, which appear in the numerical model for the computation of log mass, momentum of inertia and net volume for the floatation condition, so in all the modules included: entrainment, wood transport, wood rotation and collision. This value was not recorded during the field survey and, as a first attempt, is estimated based on the type of wood used in the experimental campaign, i.e. conifers and broadleaves, which have literature approximated values for green wood density around $700\,\mathrm{kg\,m^{-3}}$ and $800\,\mathrm{kg\,m^{-3}}$ respectively [39].

However, the wood density strongly affects buoyancy and transport [39], hence this parameter needs to be accurately chosen not to over- or under-estimate log motion. To assess how the wood density affects the numerical simulation, a second set of values is implemented, taking into account the reduction of density due to decay and its increase connected to the possible water absorption, considering also the differences among wood classes. The pictures taken during the survey prior to the simulated event show that wood was generally intact, with an almost complete bark cover, corresponding to an initial level of decay (class 1 or 2 [16]), and that was located mainly in the main channel, often partially

Table 1 Assigned Manning coefficient based on boulders size (channel) and land use

Type of area	n [$\mathrm{s\,m^{-1/3}}$]
$d_{50} < 300$ mm	0.04–0.05
$d_{50} = 300$–400 mm	0.055–0.065
Areas with boulders	0.07
Meadows	0.04
Forests	0.08

submerged under the water level. Ageing induces an average reduction of 20% of green wood density, while partial wetting may produce an increase of about 10–15%, resulting in final densities of about 610 kg m^{-3} for conifers and 700 kg m^{-3} for broadleaved wood [39].

It is worth highlighting that the proposed values present a high level of uncertainty, mainly due to the lack of information on the precise wood species and to the difficulty of estimating a posteriori wood moisture condition and decay.

2.3 Stationary hydraulic simulation

The stationary hydraulic simulation is performed with two main objectives: obtain the initial condition for the unsteady simulation and verify if the simulated water levels agree with the observations, in order to check if any error was introduced due to the domain discretization and roughness values assignment.

The simulation is performed with a constant discharge set equal to 4 m^3 s^{-1} starting with dry conditions and after about 9 hours of simulated time the flow reaches stationary conditions. Simulated water elevations are compared with the measures performed on July 5th 2012 in Fig. 5. The water levels are measured in 9 cross sections in the upstream part of the reach. No measures are available for the final 900 m. It is worth highlighting that the measured values refer to the sections surveyed on July 5th 2012, while the numerical domain combines the DTM and the specific field survey carried out on April 2015, which presents some differences from the originally surveyed sections due to morphological evolution and flooding occurred in the elapsed time.

ORSA2D_WT reproduces the 05/07/2012 flow condition with a global relative error that is about 33% of the average measured water level, 0.44 m. In the sections S1, S2, S6 and S7 the largest error is recorded. In section S7 the error is connected to the abrupt variation of the water level which implies that a small misalignment in the longitudinal coordinate corresponds to a large difference in the water level measurement (Fig. 5c). In the other three cases, the comparison of the originally surveyed cross sections and of the numerical domain reveal some mismatching of the channel morphology which may affect the water depth simulation. In the remaining cross section, the average error is 0.06 m, corresponding to a relative error of about 14%, resulting in a general acceptable agreement among measures and simulation.

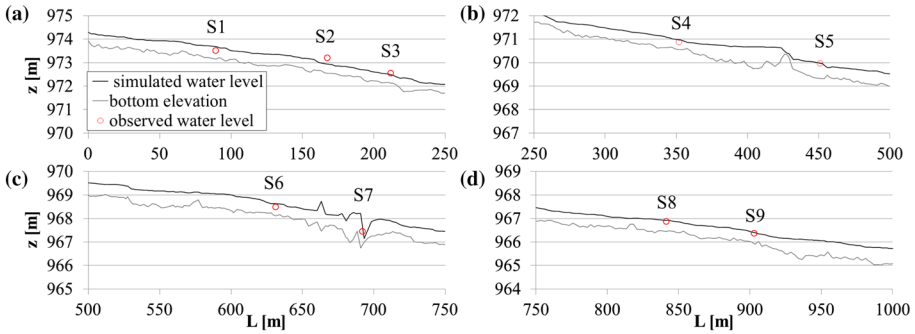

Fig. 5 Comparison of the measured (empty circles) and simulated water elevations (solid black line) for sub-reaches **a** 0–250 m, **b** 250–500 m, **c** 500–750 m, **d** 750–1000 m

3 Results

3.1 Log entrainment and displacement

According to the simulated hydrograph, the logs should start moving during the first peak, stop when the water level decreases and finally be transported again during the second peak. The comparison of the displacement of each log after the first peak (t = 1.72 h), before the second peak (t = 2.56 h) and after the second peak (t = 4 h) with the measured values is shown in Fig. 6. Most of the logs are entrained during the first event of high flow and do not move between the two peaks. Eleven of them are also remobilized by the second peak. Note that 2 logs were not found during the survey of July, 5th, so they are excluded from the final comparison. A visual comparison shows a general overestimation of log travel length. Over 70% of cases shows a simulated displacement higher than the expected value, with an error of 383 m. When the displacement is lower (the average difference being −485 m) logs are either not entrained or stop much earlier than in reality. 18% of logs are displaced with an absolute error smaller than 10 m, resulting in a good approximation of the real displacement.

On average, the observed travel distance is 249 m, against a simulated one of 384 m, once again higher than expected, while the maximum distances are similar, around 1420 m, although observed for different logs. The overestimation of the travelled distance becomes even clearer if the distribution of logs displacement is represented with a box plot (Fig. 7). The median value of the simulated displacement (188 m) is over 4 time higher than the

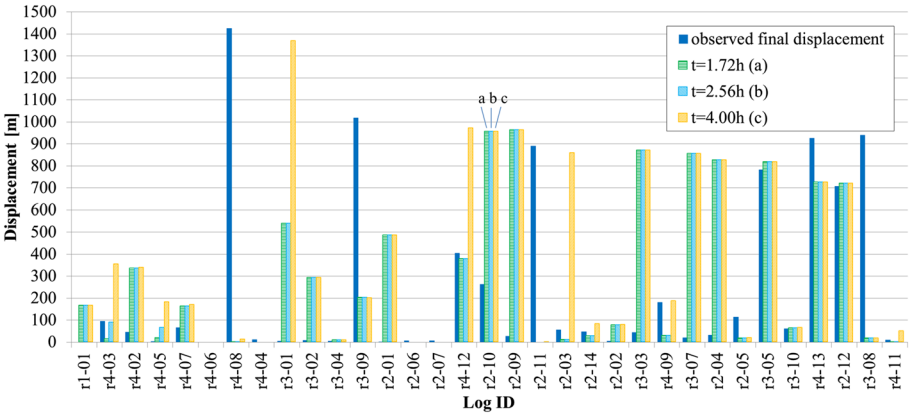

Fig. 6 Comparison of the displacement of each log

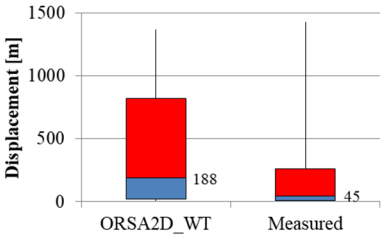

Fig. 7 Box plot of simulated and experimental displacement

median value of the measured one (45 m), and the overall distributions are not proportional, despite similar maximum and minimum values.

3.2 Effect of log shape

Logs length, diameter and slenderness generally affect the motion of cylinders. The experimental campaign showed that longer and larger pieces of wood are less mobile than the shorter ones, while a different trend is obtained from the simulation. Figure 8a shows the simulated and observed displacement distributions for logs having one dimension (either their length L or diameter D) or slenderness L / D smaller than the respective median value; in Fig. 8b the displacement is represented for logs with dimensions larger than the median values.

Displacements shown in Fig. 8a are similar, with comparable values of the medians and of the second and third quartiles, while maximum displacement is underestimated by ORSA2D_WT. On the contrary, the displacement of longer, larger or slenderer pieces of wood is strongly overestimated, as shown in Fig. 8b. The simulated median value is about 13 times the experimental one, and overall distribution is more disperse, with a standard deviation of about 420 m for the simulated displacements versus 240 m for the observations.

3.3 Effect of boulders

As shown in Sect. 2, boulders are accurately represented in the domain, with the aim of analysing their effect on the log transport. By considering the logs surveyed on July 5th, 2012, 8 were found in the areas with boulders: one at about 630 m from the initial section and the other in the second area with boulders, 5 arranged in a wood jam around a large boulder and other 2 logs in the same sub-reach. At the end of the simulation, one simulated cylinder is around 630 m from the inlet section, nearly in the same position as the measured one, and 2 are in the second area, randomly distributed around 915 m from the inlet. Figure 9 shows the observed and the simulated final logs configuration. In one case

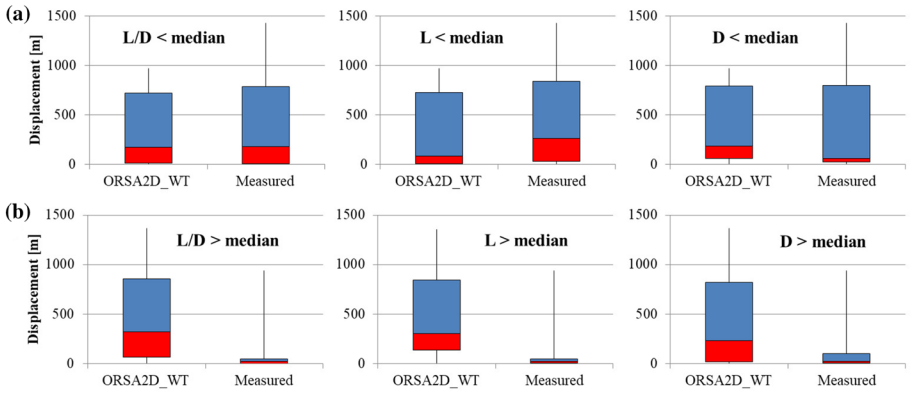

Fig. 8 Log displacement distribution for **a** logs with one dimension below the respective median value and for **b** logs with one dimension above the median value

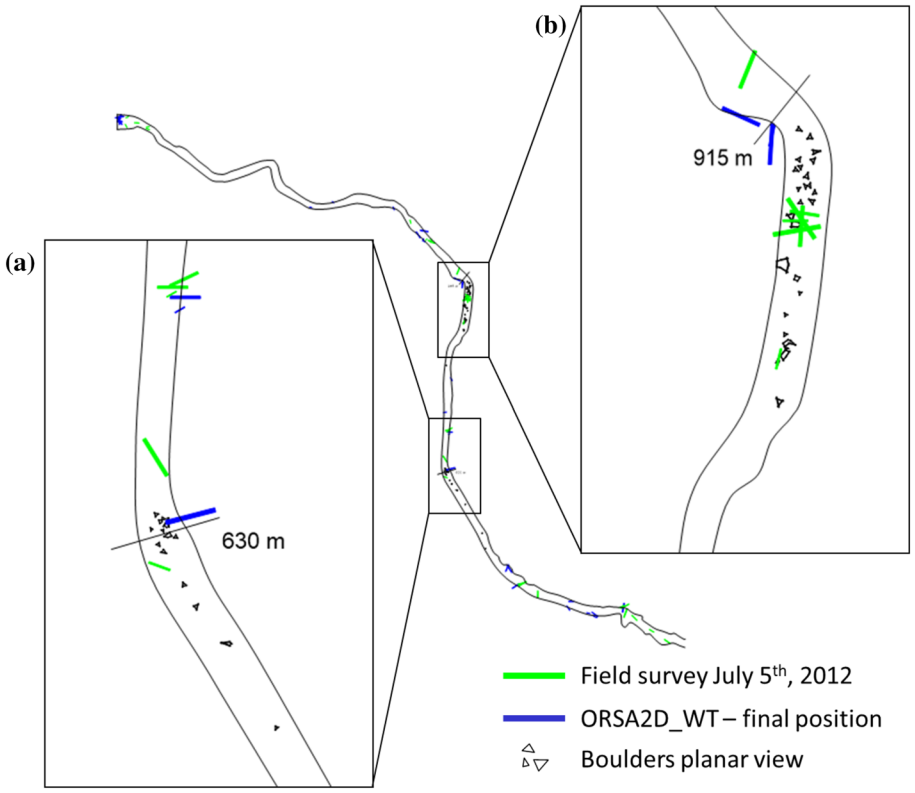

Fig. 9 Top view of the simulated reach with boulders and logs position. In the enlarged panels **a** logs in the first area with boulders and **b** logs in the second area with boulders. The length of both represented sub-reaches is about 150 m and the distances with respect to the initial cross section are displayed

(Fig. 9a) one short real log is stuck on the left side of the river, while the results of the simulation show a longer log (not the same as the one observed) which lies partially against the boulders and partially on the right riverbank. As said, both are near the same section. For the second case (Fig. 9b), real logs are leaning against boulders while simulated ones are not, since they stop on the left channel bank.

3.4 Effect of wood density

The simulation performed with the second set of density values (610 kg m^{-3} and 700 kg m^{-3}) gives different displacements and final positioning of the logs. In this case wood logs move less than those with standard higher values of density discussed in the previous paragraphs. The average displacement is 184 m (74% of the observation) and the maximum is 868 m (61% of the observation), both lower than the results of the simulation with green wood density, as can be seen by comparing Figs. 7 and 10, and than the observation. Figure 10 highlights that the distribution of simulated logs displacement is very similar to the measured one, with the second and third quartiles range that overlap those of the observations. Overall reduced wood motion is observed, which is apparently in contrast with density reduction. Considering the effect of logs

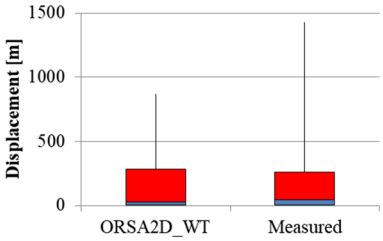

Fig. 10 Box plot of simulated and experimental displacement for the simulation with adjusted log density

characteristics, the simulated displacements are smaller and appear more consistent with the behaviour of bigger logs than with that of smaller dimension. Slenderness values are an exception, since the displacement is slightly higher for logs with blunter shape than for the slenderer ones (Fig. 11). It is worth highlighting that logs with dimensions above average always present a higher median displacement than in the observation, confirming the overestimation of larger wood motion by the model.

An additional consideration is the effect of density on the displacement for the two wood-type samples. To avoid the influence of the log characteristics, the comparison is restricted to 11 logs which have similar length and diameter (ranging from 8 to 10.5 m and from 0.27 to 0.37 m respectively), 5 of them being conifers and 6 broadleaves. Unexpectedly, field observations show that heavier logs move more than lighter ones, with a median displacement of 34 m versus 4.4 m, respectively. If the standard green wood values are considered, i.e. 700 kg m^{-3} for conifer and 800 kg m^{-3} for broadleaved wood, an opposite behaviour is observed, with broadleaves moving less than conifers (median displacement 156 m versus 485 m). For both types of wood, the simulation overestimates the cylinder movement, as it could be expected because all the logs selected for the analysis have above-median dimension and belong to the group of data in Fig. 8b. If the adjusted density values are implemented (610 kg m^{-3} and 700 kg m^{-3}), the median displacements are 23 m and 88 m for conifers and broadleaved wood, confirming a trend of higher mobility for heavier wood samples. However, measured

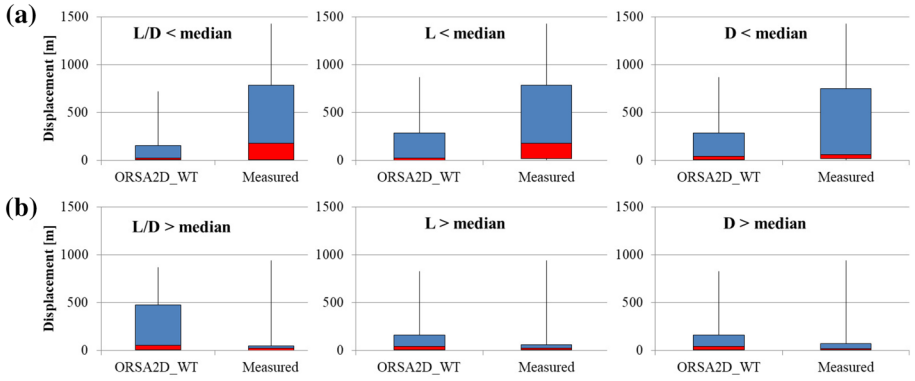

Fig. 11 Log displacement distribution for **a** logs with one dimension below the respective median value and for **b** logs with one dimension above the median value. Results of the simulation with adjusted density values

average are always smaller than simulated ones, showing that for large wood pieces the model always overestimates wood motion, independently form the density employed.

4 Discussion

4.1 Simulation with standard density values

Differences arise when comparing the observations collected during the experimental campaign and the results of the numerical model, especially on the displacement of single logs. In general, the displacement of a single piece of wood is not well represented. As shown by the statistical description in Fig. 8, the field campaign proved that longer and larger logs, on average, move less than the others. This is mainly related to the fact that their length is comparable with channel width, so they are more easily blocked by the riverbank vegetation. Besides, during the survey of July 5th, 2012, longer logs were found generally near their position surveyed on June 26th, meaning that they were nearly not entrained by the simulated high flow. On the contrary, the simulated log displacements appear nearly independent from the log dimension, showing that ORSA2D_WT overestimates the motion of larger pieces.

Moreover, the logs which jammed up against boulders and moved only a few meters in the reality, move further downstream in the simulation. The main reason for their longer displacement in the simulation can be probably ascribed to the collision model: although the restitution coefficient is calibrated for collisions in water (set equal to 0.1, i.e. assuming nearly inelastic collisions), jamming logs are not modelled as a unique static log raft, with a planar and vertical extension, but rather as a group of logs which are in touch on a 2D plane and repeatedly hit each other. This gives rise to series of weak, continuous collisions that may introduce a shifting of the logs, which then move transported by the water. To avoid the overestimation of jammed wood mobility, numerical models should take into account the interlocking of logs, including, for example, mutual friction when two logs are in touch.

The wood type-displacement relation is quite controversial, as highlighted by the results. One should expect that heavier wood pieces (broadleaves) move less than lighter ones (conifers) because of their density and weight. The simulated results (employing standard green wood density) agree with this behaviour, which however diverges from the observations. In the latter, logs with higher density are more movable than the one with similar dimension but a lower weight. The explanation for such an unexpected behaviour is not straightforward. Anchoring seems not to play a significant role, as nearly the same number of conifers and broadleaves of similar dimension were found anchored, both at boulders or at trees on the riverbanks. One possibility is the different capability of water absorption, which can vary the actual wood density. Recent literature has shown that wood density changes when wood is immersed in water and can become greater than standard values [39] for green wood and without ageing. An alternative is that heavier wood remains for longer time in the main river channel, more subject to the highest flow velocity, while conifers are more movable and easily reach the banks, where flow velocity is lower and log arrest is more probable. This option seems to be justified also by the results of the simulation with adjusted density values, which are discussed below.

It must be recognized that it is not realistic to expect that a numerical simulation could exactly track the motion of each wooden log, considering all the uncertainties related to the modelling hypotheses and those intrinsic to the physical phenomenon.

The real-scale experiment carried out in the Rienz river presents several characteristics that are not always found for standard simulations of Large wood transport, as the availability of information about wood location, the overall regularity of the channel and the *ad hoc* surveys performed. Nonetheless, some information is still lacking and contributes to the inaccuracy of the modelling, as wood density or log orientation, which was not recorded for the case of oblique configurations and was here identified from the survey pictures. Another important aspect is the initial log configuration. As displayed in Fig. 12, in most cases trees do not lay on the river bed but lean partially on the river banks with only one end in water. At present, ORSA2D_WT only considers the planar location of cylinders and, if they exit from water, no forces are exerted on them. This aspect certainly influences the log entrainment and deposition, mainly due to the lack of the friction exerted by the ground on the emerged log segment, resulting in different displacements for field and simulated wooden elements. It is thus advisable that future dynamic models for wood transport will include a friction force in addition to the drag, side, added mass and pressure gradient components, for the section of log that touches the riverbed. In addition, despite the accuracy of the implemented topography with reference to bars and boulders, simulated logs do not stop at these elements but preferably at the riverbanks. In this case, the weaknesses of the collision module, which cannot cope with jammed logs, invalidate the efforts made for the acquisition of a detailed domain, and should be carefully fixed in order to overcome this limitation.

4.2 Sensitivity to wood density values

The choice of wood density strongly affects log motion in the simulation. ORSA2D_WT accounts for wood density in all the three modules used to compute wood motion, from logs entrainment and arrest, to linear and angular acceleration computation (mass and angular momentum), and also in the collision routine (mass), as shown in Fig. 3. The results obtained with the two set of density, standard values for green wood versus adjusted values for decay and water absorption, show a lower mobility for lighter logs.

Fig. 12 Photograph of one log laying above the river bottom

This behaviour apparently contrasts with the expected one, i.e lighter bodies should be transported easier than heavier ones. However, by analysing the initiation of motion for the two simulation, we observe that the logs with adjusted density are entrainer slightly earlier and, above all, move and rotate more than in the standard simulation. Consequently, they deviate from the main flow in advance with respect to the standard density logs, reaching stable positions on the riverbanks. Heavier logs (and probably also those with standard density) remain in the flow for longer time since they possess higher inertia to motion, and for this reason can be transported for longer distances.

4.3 Overall transport dynamics

Despite the inaccuracies in the simulation of single logs displacement, which is affected mainly by the difficulties in modelling wood anchoring, a global evaluation of the performances of the model can be obtained by comparing the areas where logs are more prone to stop.

Since the simulations performed with the two set of density, green wood and adjusted values, give different displacement, the final positions occupied by the logs at the end of the two simulations are compared in Fig. 13. For both simulations, the longitudinal distribution of the simulated logs along the river is similar to the observed one, although in Fig. 13b simulated logs appear more grouped in the areas where real logs were found. Two logs, which travelled beyond the downstream boundary of the domain of the simulation, were excluded from the comparison.

To highlight the areas of deposition, the histograms in Fig. 14 present the number of logs in different sub-reaches, showing that, at the end of the considered event, a different distribution is observed according to the wood density implemented in the simulation. For the simulation with green wood density the same number of logs is found in the first three sub-reaches, while a different number is found in the last two, with most of the logs located in the final one. The presence of boulders, which are in the sub-reaches 450–650 m and 800–950 m, did not contribute to the deposition of the logs and it is our opinion that the collision scheme is the main responsible for the mismatching observed in the first simulation. When the adjusted values of density are implemented, logs tend to remain in the first four sub-reaches, with an equal or slightly higher number respect to the experiments, while 4 logs are missing in the last sub-reach. In this case more logs are found in the areas with boulders, although by observing their location it appears that they are not in touch with boulders but lie on the riverbanks. The interaction with boulders do not change much with wood density, and the higher number of logs found in these area should be connected to the tendency of lighter wood to be easily drag out of the main flow field.

In both cases, the logs found in the final sub-reach are located in the final section (Fig. 13), while the unbranched real logs are randomly distributed in this area. The analysis of aerial images shows that in the final part of the domain several boulders are found, but, since they are out of the region where the detailed survey was performed, they were not included in the simulation. This explains why real logs are well distributed in the area, although the inclusion of these boulders would not have a strong impact on the results of the simulation, due to the highlighted limitations of the collision model.

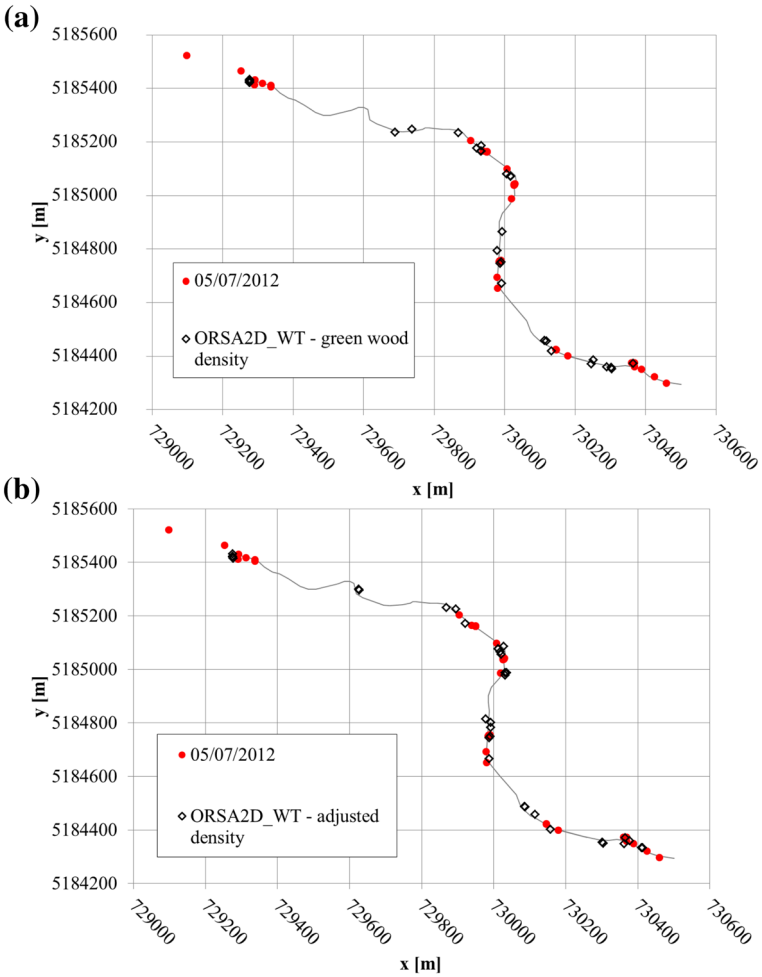

Fig. 13 Planar distribution of logs centre of mass, **a** from the survey and from the numerical simulation with standard density; **b** from the survey and from the numerical simulation with adjusted density

5 Conclusions

The first application of the Eulerian–Lagrangian model ORSA2D_WT to a real-scale case study has been here presented. The model computes wood displacement dynamically, based on the forces exerted by the flow, and is tested to assess its performances when applied to a more complex geometry than those of the flume experiments used for its calibration.

The selected case study is part of a previous experimental campaign, and provides the displacement of unbranched cylindrical logs which are compared with the results of the numerical simulation. The available dataset provides a wide range of information and is more complete than what is usually available for standard simulation. It was also expanded thanks to a specific field survey carried out on April 2015 for the acquisition of detailed topography of bars and boulders. However, wood density and logs orientation were not

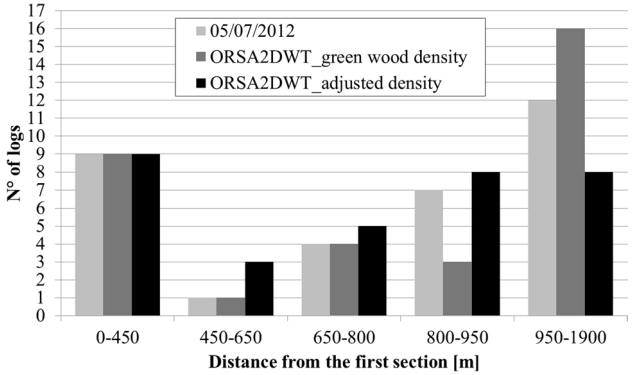

Fig. 14 Number of logs for the different sub-reaches, for the experimental campaign and the simulations with green wood and adjusted density values

recorded, so they had to be guessed on the basis of literature informations (the former) and survey pictures (the latter).

As a first attempt, the wood density is assumed equal to standard density values for green wood. Under such condition, the analysis of the effect of log length, diameter and slenderness highlights the overestimation in the simulated displacement for those cylinders whose dimensions are above the median values, while for shorter, smaller and less slender logs the measured and simulated displacements are comparable. Wood type, represented by different green wood density, affects also log motion: against expectations, field observations show that lighter logs tend to travel a shorter distance than the heavier ones, while the simulation exhibits an opposite trend.

The wood density implemented in the numerical model influences the results more than logs characteristics. By modifying density according to wood decay status and duration of wetting conditions, obtaining a reduction of density for both wood species, shorter simulated displacements are observed. This result is quite different from the expected behaviour and gives an interesting insight on the importance of such parameter for wood transport simulation. Future field work aiming at constituting a dataset for the application and calibration of wood transport models should pay much attention in measuring or estimating wood density, and real log density should be analysed carefully in order to provide additional claims for the application of numerical models to real events.

Undoubtedly, the application of the model to a real case study yields useful information about the performances of the numerical model, highlighting sensitive aspects and weaknesses which could not appear from the simulation of controlled laboratory experiments. The interaction with vegetation along the river banks, as well as the friction with the dry banks, introduces arrest mechanisms for the floating logs which are not considered by the model, but which are essential for the correct prediction of the log displacement. Moreover, the inclusion of boulders as solid obstacles in the domain appear not to affect the hydraulic simulation, which precision is mainly connected to the topography and to the roughness implemented, but their interaction with the logs is not satisfactorily represented. In the simulation, regardless of wood density, logs do not stop against boulders but on the riverbanks where the water level decreases. In general, it appears that the collision mechanism with in-stream and side obstacles is a key factor to apply successfully the numerical model to complex real cases and needs to be carefully addressed.

Nevertheless, although the numerical model does not always yield reliable results regarding the displacement of specific wood samples, it provides meaningful information of the entire wood population movement. The depositional areas are nearly the same regardless of the wood density, although some differences in the number of logs in each section, so we can say that the model can actually identify with good precision the main areas where logs tend to deposit. River managers could benefit from such instrument, detecting, for example, which areas may need more care for maintenance or in which ones the natural depositional tendency may be exploited and increased to protect downstream sites. As highlighted by the results, uncertainties are part of the phenomenon of wood transport and should be tackled by adopting a stochastic approach, for example by varying the initial wood location and orientation, or the wood density, in order to examine a wide range of scenarios and evaluate associated management strategies.

Acknowledgements We thank the Civil Protection Agency of the Autonomous Province of Bozen/Bolzano (Caterina Ghiraldo, Sandro Gius, and Bruno Mazzorana now at the Universidad Austral de Chile in Valdivia) for their collaboration in the field experiment.

References

1. Alonso CV (2004) Transport mechanics of stream-borne logs. Water Sci Appl 8:59–69
2. Andreoli A, Comiti F, Lucía A, Mazzorana B (2018) Role of channel morphology on large wood mobility in mountain rivers: a field experiment. In: Proceedings of 5th IAHR Europe congress, Trento, Italy, pp 547–548
3. Bertoldi W, Welber M, Gurnell A, Mao L, Comiti F, Tal M (2015) Physical modelling of the combined effect of vegetation and wood on river morphology. Geomorphology 246:178–187. https://doi.org/10.1016/j.geomorph.2015.05.038
4. Bocchiola D, Rulli M, Rosso R (2006) Flume experiments on wood entrainment in rivers. Adv Water Resour 29(8):1182–1195. https://doi.org/10.1016/j.advwatres.2005.09.006
5. Braudrick CA, Grant GE (2000) When do logs move in rivers? Water Resour Res 36(2):571–583. https://doi.org/10.1029/1999WR900290
6. Braudrick CA, Grant GE, Ishikawa Y, Ikeda H (1998) Dynamics of wood transport in streams: a flume experiment. Earth Surf Process Landf 22:669–683. https://doi.org/10.1002/(SICI)1096-9837(199707)22:7<669::AID-ESP740>3.0.CO;2-L
7. Buxton T (2010) Modeling entrainment of waterlogged large wood in stream channels. Water Resour Res. https://doi.org/10.1029/2009WR008041
8. Chow CY (1979) An introduction to computational fluid mechanics. Wiley, New York
9. Comper T, Picco L, Bladé E, Ruiz-Villanueva V (2018) Numerical modelling of large wood dynamics in the braided Piave River (Italy): the important role of roots. In: Proceedings of 5th IAHR Europe congress, Trento, Italy, pp 557–558
10. Cowan WL (1956) Estimating hydraulic roughness coefficients. Agric Eng 37(7):473–475
11. Crook D, Alistar R (1999) Relationships between riverine fish and woody debris: implications for lowland rivers. Mar Freshw Res. https://doi.org/10.1071/MF99072
12. Crosato A, Rajbhandari N, Comiti F, Cherradi X, Uijttewaal W (2013) Flume experiments on entrainment of large wood in low-land rivers. J Hydraul Res. https://doi.org/10.1080/00221686.2013.796573
13. De Cicco P, Paris E, Ruiz-Villanueva V, Solari L, Stoffel M (2018) In-channel wood-related hazards at bridges: a review. River Res Appl. https://doi.org/10.1002/rra.3300
14. Diehl TH (1997) Potential drift accumulation at bridges. US Department of Transportation, Federal Highway Administration Research and Development, Turner-Fairbank Highway Research Center
15. Gasser E, Simon A, Perona P, Dorren L, Hübl J, Schwarz M (2018) Quantification of potential recruitment of large woody debris in mountain catchments considering the effects of vegetation on hydraulic and geotechnical bank erosion and shallow landslides. In: E3S web of conferences, vol 40, p 02046. https://doi.org/10.1051/e3sconf/20184002046
16. Harmon M, Woodall C, Fasth B, Sexton J (2008) Woody detritus density and density reduction factors for tree species in the united states: a synthesis. USDA Forest Service, Northern Research Station, general technical report NRS29

17. Hecker C (1997) Physics, part 3: collision response. Game Developer Magazine, pp 11–18
18. Keller EA, Swanson FJ (1979) Effects of large organic material on channel form and fluvial processes. Earth Surf Process 4(4):361–380. https://doi.org/10.1002/esp.3290040406
19. Kimura I, Kitazono K (2018) Studies on driftwood motions around obstacles by laboratory and numerical experiments. In: E3S web of conferences, vol 40. https://doi.org/10.1051/e3sconf/20184002032
20. Lagasse P (2010) Effects of debris on bridge pier scour. The National Academies Press, Washington, DC https://doi.org/10.17226/22955
21. Lassettre NS, Kondolf GM (2012) Large woody debris in urban stream channels: redefining the problem. River Res Appl 28(9):1477–1487. https://doi.org/10.1002/rra.1538
22. Lenzi M, Picco L, Bettella F (2015) Sediment management (including large wood). ETC project SedAlp, sediment management in Alpine basins
23. Lucía A, Antonello A, Campana D, Cavalli M, Crema S, Franceschi S, Marchese E, Niedrist M, Schneiderbauer S, Comiti F (2015) Monitoring and modeling large wood recruitment and transport in a mountain basin of north-eastern Italy. Eng Geol Soc Territ. https://doi.org/10.1007/978-3-319-09054-2-31
24. Mazzorana B, Comiti F, Volcan C, Scherer C (2011) Determining flood hazard patterns through a combined stochastic-deterministic approach. Nat Hazards 59:301–316. https://doi.org/10.1007/s11069-011-9755-2
25. Mazzorana B, Hübl J, Zischg A, Largiader A (2011) Modelling woody material transport and deposition in Alpine rivers. Nat Hazards 56(2):425–449. https://doi.org/10.1007/s11069-009-9492-y
26. Mazzorana B, Ruiz-Villanueva V, Marchi L, Cavalli M, Gems B, Gschnitzer T, Mao L, Iroumé A, Valdebenito G (2018) Assessing and mitigating large wood-related hazards in mountain streams: recent approaches. J Flood Risk Manag 11(2):207–222. https://doi.org/10.1111/jfr3.12316
27. Persi E (2018) Eulerian–Lagrangian modelling of large floating debris transport during floods. Dissertation, Department of Civil Engineering and Architecture Faculty of Engineering, University of Pavia
28. Persi E, Petaccia G, Sibilla S (2018) Large wood transport modelling by a coupled Eulerian–Lagrangian approach. Nat Hazards 91(1):59–74. https://doi.org/10.1007/s11069-017-2891-6
29. Persi E, Petaccia G, Sibilla S, Brufau P, García-Navarro P (2018) Calibration of a dynamic Eulerian–Lagrangian model for the computation of wood cylinders transport in shallow water flow. J Hydroinform 21(1):164–179. https://doi.org/10.2166/hydro.2018.085
30. Persi E, Petaccia G, Fenocchi A, Manenti S, Ghilardi P, Sibilla S (2019) Hydrodynamic coefficients of yawed cylinders in open-channel flow. Flow Meas Instrum 65:288–296. https://doi.org/10.1016/j.flowmeasinst.2019.01.006
31. Petaccia G, Soares-Frazão S, Savi F, Natale L, Zech Y (2009) Simplified versus detailed two-dimensional approaches to transient flow modeling in urban areas. J Hydraul Eng 136(4):262–266. https://doi.org/10.1061/(ASCEHY).1943-7900.0000154
32. Petaccia G, Leporati F, Torti E (2016) OpenMP and CUDA simulations of Sella Zerbino Dam break on unstructured grids. Comput Geosci 20(5):1123–1132. https://doi.org/10.1007/s10596-016-9580-5
33. Petaccia G, Persi E, Sibilla S, Brufau P, García-Navarro P (2018) Enhanced one-way coupled SWE-DE model for floating body transport. IJEGE. https://doi.org/10.4408/IJEGE.2018-01.S-15
34. Piégay H, Gurnell A (1997) Large woody debris and river geomorphological pattern: examples from S.E. France and S. England. Geomorphology 19(1):99–116. https://doi.org/10.1016/S0169-555X(96)00045-1
35. Ravazzolo D, Mao L, Picco L, Lenzi M (2015) Tracking log displacement during floods in the Tagliamento river using RFID and GPS tracker devices. Geomorphology 228:226–233. https://doi.org/10.1016/j.geomorph.2014.09.012
36. Ruiz-Villanueva V, Bladé E, Sánchez-Juny M, Marti-Cardona B, Díez-Herrero A, Bodoque JM (2014) Two-dimensional numerical modeling of wood transport. J Hydroinform 16(5):1077. https://doi.org/10.2166/hydro.2014.026
37. Ruiz-Villanueva V, Bodoque JM, Díez-Herrero A, Bladé E (2014) Large wood transport as significant influence on flood risk in a mountain village. Nat Hazards 74(2):967–987. https://doi.org/10.1007/s11069-014-1222-4
38. Ruiz-Villanueva V, Díez-Herrero A, Ballesteros-Canovas J, Bodoque J (2014) Potential large woody debris recruitment due to landslides, bank erosion and floods in mountain basins: a quantitative estimation approach. River Res Appl 30:81–97. https://doi.org/10.1002/rra.2614
39. Ruiz-Villanueva V, Piégay H, Gaertner V, Perret F, Stoffel M (2016) Wood density and moisture sorption and its influence on large wood mobility in rivers. CATENA 140:182–194. https://doi.org/10.1016/j.catena.2016.02.001

40. Ruiz-Villanueva V, Wyżga B, Mikuś P, Hajdukiewicz M, Stoffel M (2017) Large wood clogging during floods in a gravel-bed river: the Długopole bridge in the Czarny Dunajec river, Poland. Earth Surf Process Landf 42(3):516–530. https://doi.org/10.1002/esp.4091
41. Schalko I (2017) Large wood accumulation probability at a single bridge pier. In: Proceedings of 37th IAHR world congress, Kuala Lumpur, Malaysia. https://doi.org/10.3929/ethz-b-000185312
42. Schmocker L, Hager WH (2011) Probability of drift blockage at bridge decks. J Hydraul Eng 137(4):470–479. https://doi.org/10.1061/(ASCE)HY.1943-7900.0000319
43. Shrestha B, Nakagawa H, Kawaike K, Baba Y, Zhang H (2012) Driftwood deposition from debris flows at slit-check dams and fans. Nat Hazards 61:577–602. https://doi.org/10.1007/s11069-011-9939-9
44. Stockstill RL, Daly SF, Hopkins MA (2009) Modeling floating objects at river structures. J Hydraul Eng 135(5):403–414. https://doi.org/10.1061/(ASCE)0733-9429(2009)135:5(403)